Pergamon

Ocean Engineering 29 (2002) 261–278

OCEAN ENGINEERING

Applied hydrodynamic wave-resistance computation by Fourier transform

Jorge D'Elia *, Mario A. Storti, Sergio R. Idelsohn

Centro Internacional de Métodos Computacionales en Ingeniería (CIMEC) INTEC (UNL-CONICET), Güemes 3450, 3000-Santa Fe, Argentina

Received 8 September 2000; accepted 4 October 2000

Abstract

An applied Fourier transform computation for the hydrodynamic wave-resistance coefficient is shown, oriented to potential flows with a free surface and infinity depth. The presence of a ship-like body is simulated by its equivalent pressure disturbance imposed on the un-perturbed free surface, where a linearized free surface condition is used. The wave-resistance coefficient is obtained from the wave-height downstream. Two examples with closed solutions are considered: a submerged dipole, as a test-case, and a parabolic pressure distribution of compact support. In the three dimensional case, a dispersion relation is included which is a key resource for an inexpensive computation of the wave pattern far downstream like fifteen ship-lengths.

Keywords: Free surface flows; Hydrodynamics; Fluid dynamics; Computational techniques; Mathematical methods in physics

1. Introduction

When a body moves near the free surface of a fluid, a pattern of trailing gravity waves is formed. The energy spent in building this pattern comes from the work done by the body against the wave resistance. As a first approximation, the wave resistance can be computed with a potential model, whereas for the viscous drag it can be assumed that the position of the surface is held fixed at the reference hydro-

* Corresponding author. Tel.: +54-342-4559175; fax: +54-342-4550944.
E-mail addresses: jdelia@trantor.arcride.edu.ar (J. D'Elia), mstorti@intec.unl.edu.ar (M.A. Storti), rnsergio@arcride.edu.ar (S.R. Idelsohn).

0029-8018/01/$ - see front matter
PII: S0029-8018(00)00073-1

static position, i.e. a plane. This is, basically, the Froude hypotheses. With this assumption, we are neglecting the interaction produced by the boundary layer, which tends to produce a larger body, whose wave pattern, in turn, tends to modify the potential flow which is the input to the boundary layer process. Even if a potential model is assumed for the liquid, the problem is non-linear due to the free surface boundary condition. Potential methods are classical and widely accepted for calculating several kind of flow configurations, e.g. see Morino (1985) and D'Elía et al. (2000a,b,c,d). In some problems a two-dimensional approach is sufficient, for instance, flows past multicomponent airfoils, infinite cascade and ground effects, e.g. see Mokry (1990) and Storti et al. (1995), and it is an interesting case due to the possibility of using analytic functions of complex variable, which allows an elegance of treatment.

Methods for determining the wave-resistance force generated by a moving ship-like body is an old problem in ship hydrodynamics, whose history stretches back over 100 years. Today, several analytical and semi-analytical strategies for determining the wave resistance by a moving ship-like body with potential models are available, e.g. see Wehausen and Laitone (1960) and Wehausen (1973) for an extensive review (where 16 pages of authors references are given) or, more recently, Miloh (1991) and Larsson and Baba (1996). Notwithstanding, a short review follows, where modern CFD approaches, like finite and boundary elements, are omitted. As is well known, potential linearized wave-resistance theories can be applied for relatively slender ships, and they are often used for hull improvement, for instance, container ships at high speeds. These theories are closely related on the Michell's integral and its modified forms, e.g. see Weinblum (1930), Karp et al. (1960), Maruo and Bessho (1963) and Inui (1962), while simplified expressions are based on slender ship theories, e.g. see Wyatt and Chang (1994). For catamarans see Papanikolaou and Androulakakis (1991), Min (1992) and Suzuki (1993). The reduction of ship waves for the preservation of river banks was studied by Doctors et al. (1991), while Noblesse and Gagan (1976) proposed a non-linear theory by continuous mapping. Nevertheless, thin ship theories are not applicable for full hulls, such as a tanker in ballast condition, so many efforts have been made to improve linearized wave-resistance theories, e.g. see Ogilvie (1968), Newman (1976), Raven (1996) and D'Elía (1997), where linearized freesurface conditions are formulated on the basis of a double body flow around the ship-like body (the double body flow). In an infinitely deep and unbounded fluid, standard procedures for the solution of the Michell integral involve the use of Fourier series/integral or Green function theory, for instance, Wehausen (1973) treats a linearized moving deeply submerged body by the last method. Not all these flow problems can be solved with an equivalent effort, for instance, a separable coordinate system must be used in the Fourier methods and, then, the boundary conditions are imposed on one of the surface coordinates. On the other hand, Chang and Chwang (1997) have been studying the wave pattern of a moving source, in a viscous fluid of infinite depth, by the use of the Fourier transform, whose solutions, which satisfy linearized free surface conditions, possess some characteristics of the classical Kelvin ship wave pattern. As a first simplification, the presence of the body can be simulated by its equivalent pressure disturbance, of compact support, on the

free surface. Some of the motions which can arise under simple surface pressure are discussed, by example, by Lamb (1945). Lamb's presentation is well known but, as Stoker remarks, assumes fictitious damping forces in order to be rid of the free oscillations and thus obtain a unique solution.

In this work, an applied Fourier computation of the wave-resistance over a ship-like body in steady motion is made, by means of a potential flow model with a linearized free surface boundary condition and infinity depth. The presence of the body is simulated by an equivalent pressure disturbance of compact support on the free surface. The analytical and semi-analytical solutions that can be obtained by this alternative method can be used to test other numerical algorithms such as those based, for instance, on finite differences, finite elements or boundary elements. In particular, we have used it to test finite element and panel codes coupled with a Discrete Non-Local (DNL) absorbing boundary condition, e.g. see Storti et al. (1998a,b, 2000) and Bonet et al. (1998). Also, in the extension to the three dimensional case, a dispersion relation is found as a key element for an inexpensive computation of the wave pattern far downstream, for instance, fifteen ship-lengths, as is described in a previous work, see D'Elía et al. (2000a,d).

2. Computation of the velocity potential by contour integration

The linearized governing equation system for the perturbation velocity potential $\phi(x, z)$ of an inviscid and incompressible flow with a pressure perturbation $P(x)$ on its free surface is, e.g. see Stoker (1957),

$$\begin{cases} \phi_{,xx}+\phi_{,zz}=0 & \text{in } z<0; \\ \phi_{,z}+K^{-1}\phi_{,xx}=P_{,x}U/(\rho g) & \text{at } z=0; \end{cases} \tag{1}$$

with $-\infty<x<+\infty$, where $K=g/U^2$ is the characteristic wavenumber, U is the free-stream speed, g is the gravity acceleration and ρ is the fluid density. The z-axis is parallel to the upstream non-perturbed velocity U and the z-axis positive upwards. The Froude number is defined as $Fr=U/\sqrt{gL}$, where L is a characteristic length of the flow problem and is related to the characteristic wave-number by $Fr=1/\sqrt{KL}$. In addition, we will assume that the pressure perturbation P has compact support.

One word about the pressure perturbation $P(x)$. As is well known, perturbation techniques are often employed to solve two and three dimensional potential flows with a free surface. For instance, from these techniques we obtain the thin, slender and slow ship cases, e.g. see Wehausen (1973) or Ohkusu (1996). In any case, quasi-linearized approximations are obtained by substituting $\Phi=\Phi\Phi_o+\phi$ and neglecting terms $O(\phi^2)$, where Φ is the total potential velocity. For flows with past-submerged or floating bodies, Φ_o the rigid wall, or double body, potential solution satisfying the homogeneous Neumann boundary condition $\partial_y\Phi_o=0$ at the hydrostatic equilibrium plane ($z=0$), whereas ϕ is the perturbation potential satisfying a perturbed system equation, where its free surface condition is related to a Neumann boundary condition with a source term proportional to the streamlined second derivative of the rigid-

wall potential Φ_o. On the other hand, for submerged bodies this perturbed Neumann boundary condition can be replaced by an equivalent pressure load distribution imposed on $z=0$, which is caused by the presence of the body in the flow. Then, in these cases, we can solve a simpler perturbed flow problem, where the submerged body is replaced by its equivalent pressure distribution imposed at the hydrostatic equilibrium plane. Also, some hovercraft-like flow problems can be included in this approach. Going back to Eq. (1) for its solution we employ the pair-Fourier transform

$$f(x,z)=\int_{-\infty}^{\infty} ds\hat{e}^{+isx}\hat{f}(s,z); \tag{2}$$

$$\hat{f}(s,z)=\frac{1}{2\pi}\int_{-\infty}^{\infty} dxe^{-isx}f(x,z); \tag{3}$$

where $f\equiv\phi$ (velocity potential) or $f\equiv P$ (surface pressure). Replacing (2) in the Laplace Eq. (1) results

$$\frac{d^2\hat{\phi}}{dz^2}-s^2\hat{\phi}=0 \quad \text{for } z<0; \tag{4}$$

whose solution is $\hat{\phi}(s,z)=Ce^{|s|z}$, for $z\leq 0$. Performing the Fourier transform in Eq. (1b), we have

$$\frac{d\hat{\phi}}{dz}-\frac{s^2}{K}\hat{\phi}-\frac{isU}{\rho g}\hat{P}=0 \quad \text{for } z=0; \tag{5}$$

introducing the solution $\hat{\phi}(s,z)$ in Eq. (4) it follows that the Fourier transform of the velocity potential is

$$\hat{\phi}(s,z)=H(s)\hat{P}(s,z); \tag{6}$$

where

$$H(s)=\frac{iU}{\rho g}\frac{s}{|s|-K^{-1}s^2}; \tag{7}$$

is a transfer function in the complex plane. Introducing Eq. (6) in the Fourier Transform Eq. (2), we conclude that

$$\phi(x,0)=\frac{iU}{\rho g}\int_{-\infty}^{\infty} ds\frac{se^{isx}}{|s|-K^{-1}s^2}\hat{P}(s,0); \tag{8}$$

where $\hat{P}(s,0)$ is analytic on the complex plane s, so we can consider Eq. (8) as a contour integral over the complex s-plane. The factor e^{isx} is also analytic, whereas for the kernel $H(s)=s/(|s|-K^{-1}s^2)$, we first have to define how $|s|$ is extended to the whole complex plane. A natural way is with a branch-cut on the imaginary axis

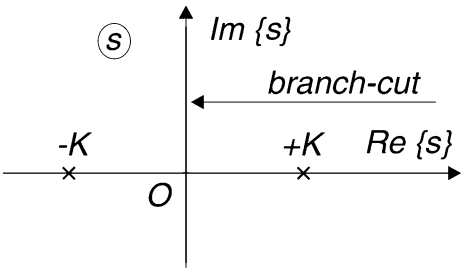

Fig. 1. The kernel $H(s)$ has a branch-cut over the imaginary axis and two poles at $s=\pm K$.

$$|s|=\begin{cases}+s & \text{if } Re(s)>0;\\ -s & \text{if } Re(s)<0.\end{cases} \tag{9}$$

Then, the transformed velocity potential $\hat{\phi}(s,0)$ also has a branch-cut on the imaginary axis and two isolated poles at $s=\pm K$, see Fig. 1. But, the integration path for Eq. (8) is on the real axis and then passes over the two poles, so we have to define how we consider the residues at them. If we consider that the path passes through the center of the pole and P is symmetric, then $\phi(x, 0)$ is also symmetric, which is an incorrect result, so we consider the integral over a path P^- with the poles on the left, see Fig. 2. In the first place let us consider the integral for $x<0$, where we deform the integration contour to path $P^-_{(-\delta)}$, composed of four sub-paths $P^-_{(-\delta)}=BC+CO+OC'+C'B'$, see Fig. 3. Note that we also include the path COC' around the cut. The contribution of the two segments BC and $C'E'$ is

$$|e^{isx}|=e^{-|s''||x|}<e^{-\delta|x|}; \tag{10}$$

where $s''=\mathrm{Im}(s)<-\delta$, so the contribution of the first path $BC+C'B'$ tends to $C_1\, e^{-\delta|x|}$. On the other hand, the contribution of the second path $CO+OC'$ can be estimated as $C_2\delta$, since Eq. (6), and then

$$\phi(x,0)\leq C_1 e^{-\delta x}+C_2\delta. \tag{11}$$

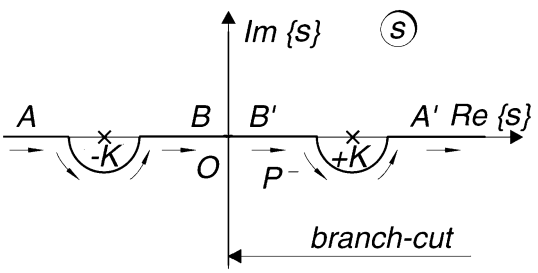

Fig. 2. Integration path P^- leaving the poles on the left.

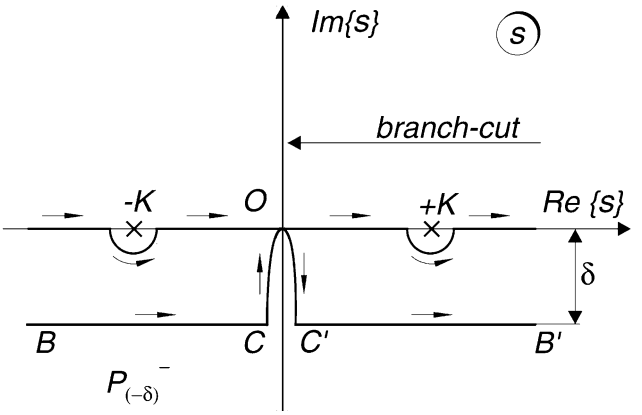

Fig. 3. Integration path $P^{-}_{(-\delta)}$, leaving the poles on the left and for $x<0$.

Taking $\delta=|x|^{-1/2}$ we have $\phi(x,0)\rightarrow 0$ when $x\rightarrow-\infty$ (upstream). Next, let us consider the case $x>0$ (downstream). The path is now $P^{-}_{(+\delta)}$, see Fig. 4. As is usual in complex theory, the contributions around the poles are equivalent to their residues. On the other hand, the contribution of the paths ABO and $OB'A'$ can be estimated as before, so they tend to zero for $x\rightarrow+\infty$, whereas the contribution of the residues are

$$\int_{P_{(+k)}+P_{(-k)}} dsH=2\pi i[\mathrm{Res}\{H,+K\}+\mathrm{Res}\{H,-K\}]; \tag{12}$$

On a neighborhood of $s=\pm K$, the poles are in the denominator ($|s|-K^{-1}s^2$) which are written now as

$$|s|-K^{-1}s^2=-\frac{s}{K}(s\mp K); \tag{13}$$

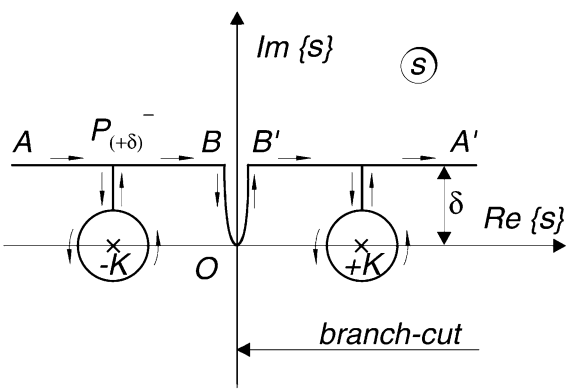

Fig. 4. Integration path $P^{-}_{(+\delta)}$, leaving the poles on the left and for $x>0$.

and then

$$\mathrm{Res}\{H,\pm K\}=-\frac{iKU}{\rho g}\,e^{\pm ikx}\hat{P}(\pm K) \tag{14}$$

Thus we have

$$\phi(x,0)=Ae^{+iKx}\hat{P}(+K)+Ae^{-iKx}\hat{P}(-K); \tag{15}$$

where $A=2\pi KU/(\rho g)=2\pi/\rho U$. In brief, the solution for a path such as the P^-, see Fig. 2, is of the form

$$\phi(x,0)=\begin{cases}0 & \text{for } x\longrightarrow-\infty;\\ 2ARe\{e^{iKx}\hat{P}(K)\} & \text{for } x\longrightarrow+\infty;\end{cases} \tag{16}$$

where $\hat{P}(-K)=\overline{\hat{P}(-K)}$, since $P(x)$ is real. If we used an integration path leaving the poles on the right, the solution would be

$$\phi(x,0)=\begin{cases}2ARe\{e^{iKx}\hat{P}(K)\} & \text{for } x\longrightarrow-\infty;\\ 0 & \text{for } x\longrightarrow+\infty.\end{cases} \tag{17}$$

But, we know that the solution with physical sense is the first case, so the correct integration path is P^-. That is, the appropriated branch-cut and integration contour are selected from agreement with the experimental observation (waves downstream only). On the other hand, this selection is equivalent to the well known Sommerfeld radiation condition (the waves should behave at infinity like progressive waves moving away from the source), e.g. see Stoker (1957). Alternatively, one can show that the integration path P^- is the correct one by adding a small diffusive term, or Rayleigh artificial viscosity term, and in such a case the poles move to the $\mathrm{Im}\{s\}>0$ semi-plane, so the integral in Eq. (8) can be taken straightforwardly on the real axis, i.e. leaving both poles on the left. It is easy to show, then, that letting the diffusive term tend to zero is equivalent to deform the integration path as P^-. This artifice is widely regarded as a reliable way to satisfy the radiation boundary conditions. For instance, if there is no pressure perturbation, the linearized free-surface boundary condition (1) reduces to

$$\phi_{,xx}+K\phi_{,z}=0 \text{ at } z=0; \tag{18}$$

This boundary condition is invariant under longitudinal coordinate inversion $x\longrightarrow -x$ and, so, it would give either a symmetric solution or an ill posed problem. This is corrected through the addition of a Rayleigh artificial viscosity term

$$\phi_{,xx}+K\phi_{,z}+\nu\phi_{,x}=0 \text{ at } z=0 \tag{19}$$

where ν is the Rayleigh viscosity parameter. On the other hand, in the numerical solution of Eq. (18) by finite-differences techniques, the symmetry is broken by means of upwind-like operators which are equivalent to the numerical solution of Eq. (19). A very comprehensive analysis about this topic is given by Letcher (1993),

and an extension is made by D'Elía et al. (2000a,d). Going back to Eq. (17), the elevation η is then obtained from, e.g. see Wehausen (1973) or Landweber (1961)

$$\eta = -\frac{U\partial\phi}{g\,\partial x} = -\frac{4\pi}{\rho g} Re[iKe^{iKx}\hat{P}(K)]; \tag{20}$$

$$\eta = \frac{4\pi}{\rho U^2} \mathrm{Im}[e^{iKx}\hat{P}(K)]; \tag{21}$$

and the (maximum) wave height is

$$\bar{\eta} = \frac{4\pi}{\rho U^2}|\hat{P}(K)| \quad \text{for } x \to \infty. \tag{22}$$

It is well known that the wave resistance is directly related to the amplitude downstream but we will give an alternative derivation.

3. Computation of the wave resistance by contour integration

The wave resistance for transversal unit area is given by

$$F_x = \int_{-\infty}^{\infty} P dx \frac{\partial \eta}{\partial x} = = \int_{-\infty}^{\infty} P dx \frac{\partial}{\partial x}\left[\frac{P}{\rho g} - \frac{U}{g}\frac{\partial \phi}{\partial x}\right]. \tag{23}$$

The contribution of the first term is null since we assume that P has compact support, so

$$F_x = -\frac{U}{g}\int_{-\infty}^{\infty} dx P\phi_{,xx}; \tag{24}$$

but from Eq. (8)

$$\frac{\partial^2 \phi}{\partial x^2} = \int_{p^-} ds\, e^{+isx} F(s)\hat{P}(s); \tag{25}$$

where

$$F(s) = \frac{U}{\rho g}\frac{(is)^3}{|s| - K^{-1}s^2}; \tag{26}$$

replacing $\hat{P}(s)$ by its Fourier inverse transform (3) we have

$$\frac{\partial^2 \phi}{\partial x^2} = \int_{-\infty}^{\infty} dx' G(x - x')P(x'); \tag{27}$$

where

$$G(\pm\xi)=\frac{1}{2\pi}\int_{p-} ds e^{\pm is\xi} F(s); \tag{28}$$

is a function on the complex plane. Next, let us decompose this function G as

$$G(\xi)=G_a(\xi)+G_s(\xi); \tag{29}$$

where $G_{s/a}$ are its symmetric and antisymmetric components, respectively. In Appendix A we show that the antisymmetric part does not contribute to the wave resistance computation, so

$$F_x=-\frac{U}{g}\int\int P(x)G_s(x-x')P(x')dxdx'; \tag{30}$$

and that the symmetric part, on the transformed plane, is given by

$$G_s(\xi)=i\,\mathrm{Res}\{F(s),+K\}\cos(K\xi) \tag{31}$$

where we still have to evaluate the residue, but with Eq. (13), we have

$$\mathrm{Res}\{F,K\}=\frac{U}{\rho g}\lim_{s\to K}(s-K)\frac{(is)^3}{|s|-K^{-1}s^2}=\frac{iK^3u}{\rho g}. \tag{32}$$

Replacing in Eq. (31) we obtain

$$G_s(\xi)=-\frac{K^2}{\rho U}\cos(K\xi); \tag{33}$$

inserting this results in Eq. (30)

$$F_x=\frac{K^2}{\rho g}\int_{-\infty}^{\infty} P(x)P(x')\cos K(x-x')\,dx\,dx'. \tag{34}$$

Since $\sin(K\xi)$ is skew-symmetric, we can replace the cosine by the complex exponential

$$F_x=\frac{K^2}{\rho g}\int_{-\infty}^{\infty} P(x)P(x')e^{iK(x-x')}\,dx\,dx'; \tag{35}$$

or

$$F_x=\frac{4\pi^2K^2}{\rho g}|\hat{P}(K)|^2 \tag{36}$$

where $\hat{P}(K)$ is the Fourier transform of the pressure disturbance. On the other hand, the wave resistance, Eq. (36), can be written in terms of the wave amplitude $\bar{\eta}$, Eq. (22), as

$$F_x=\frac{1}{4}\rho g\bar{\eta}^2; \tag{37}$$

in agreement with classical results, for instance, see Landweber (1961). Thus, we have a derivation of the wave resistance by means of the Fourier transform of the pressure disturbance, imposed on the unperturbed free surface, and its residues around the poles in the complex plane, where only the symmetric part of the G function contributes to its value.

4. Two examples with closed solutions

4.1. Submerged dipole

This is a rederivation of a known result, as a test case. The complex potential of a submerged dipole (or infinitesimal cylinder) at a depth f with respect to the surface $z=0$ is

$$\phi(t) = \frac{U^2b}{t+if} + \frac{U^2b}{t-if}; \tag{38}$$

where $t=x+iz$ is the complex variable, U^2b is the dipole intensity, so a submerged cylinder of radius b can be replaced by a dipole of intensity U^2b in the limit of a very small radius. The velocity field is $w=u-iv=d\phi/dt$ or

$$w=-\frac{U^2b}{(t+if)^2} - \frac{U^2b}{(t-if)^2}. \tag{39}$$

For the wave resistance computation we need its value on the plane $z=0$, with $P(x)=\rho bw$, so

$$P(x)=-\frac{\rho U^2b^2}{(x+if)^2}-\frac{\rho U^2b^2}{(x-if)^2}; \tag{40}$$

and its Fourier transform is

$$\hat{P}(s)=-\frac{\rho U^2b^2}{2\pi}\int_{-\infty}^{\infty} dx\left[\frac{1}{(x+if)^2}+\frac{1}{(x-if)^2}\right]e^{-isx}. \tag{41}$$

This expression can be considered as a contour integral on the complex plane t, where $\hat{P}(0)=0$ (Fig. 5). For $s<0$ we chose an integration path P on a straight line AB, so we have $z=\mathrm{Im}(t)=\mathrm{cnst}>0$ and

$$|e^{ist}|=e^{-|s|z}; \tag{42}$$

so the integral tends to zero for $z\to\infty$, then

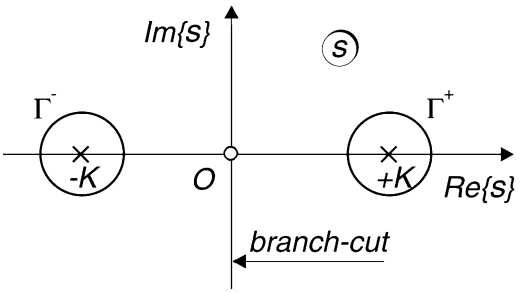

Fig. 5. Integration path Γ around the poles.

$$\begin{aligned}\hat{P}(s) &= -i\rho U^2 b^2 \mathrm{Res}\left\{\frac{e^{-ist}}{(t-if)^2}, if\right\}\\ &= -i\rho U^2 b^2 \mathrm{Res}\left\{\frac{e^{-is(t-if)}}{(t-if)^2} e^{sf}, if\right\}\\ &= -i\rho U^2 b^2 e^{sf} \mathrm{Res}\left\{\frac{e^{-is\xi}}{\xi^2}, 0\right\}\\ &= -i\rho U^2 b^2 e^{sf} \mathrm{Res}\left\{\frac{1-is\xi+\cdots}{\xi^2}, 0\right\}\\ &= -\rho U^2 b^2 s e^{sf}.\end{aligned} \tag{43}$$

Since P is real and even, then $\hat{P}(s)$ too, so the Fourier transform for all s is

$$\hat{P}(s) = \rho U^2 b^2 |s| e^{-|s|f}; \tag{44}$$

replacing in Eq. (37) and defining the non-dimensional wave-resistance coefficient as $C_w = F_x/\rho U^2 b$ we obtain

$$C_w = \frac{1}{\rho U^2 b} \frac{4\pi^2 K^2}{\rho g} \rho^2 U^4 b^4 K^2 e^{-2Kf}; \tag{45}$$

$$C_w = 4\pi^2 \left(\frac{b}{f}\right)^3 \left(\frac{f}{K^{-1}}\right)^3 e^{-2f/K^{-1}}; \tag{46}$$

which is a classical expression, for instance, see Landweber (1961) and Lamb (1945). In this case, the pressure perturbation has not compact support, i.e. it extends to infinity; however, it decays $\propto |x|^{-2}$. In Fig. 6 we show the plot of this analytical wave-resistance coefficient as a function of the Froude number, compared with a finite element solution, e.g. see Storti et al. (1998a,b, 2000).

4.2. Parabolic pressure distribution of compact support

As a second example, let us consider a parabolic pressure distribution of compact support

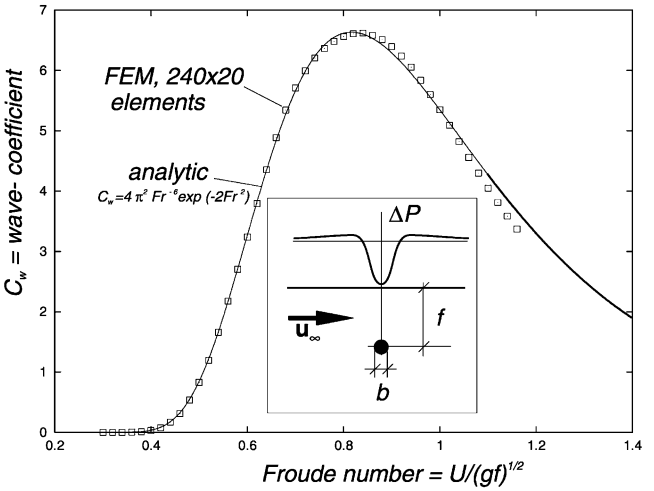

Fig. 6. Wave-resistance coefficient for a submerged dipole.

$$P=\begin{cases}\overline{\Delta P}[1-(x/a)^2] & \text{for } |x|<a;\\ 0 & \text{for } |x|>a.\end{cases} \tag{47}$$

Its Fourier transform is

$$\hat{P}(s)=-4a\overline{\Delta P}\frac{sa\cos sa-\sin sa}{(sa)^3}; \tag{48}$$

where $\hat{P}(0)=4a\overline{\Delta P}/3$ is finite; see Fig. 7. The induced wave resistance is, replacing in Eq. (37),

$$F_x=\frac{16(Ka)^2\overline{\Delta P}^2}{\rho g}\left[\frac{Ka\,\cos Ka-\sin Ka}{(Ka)^3}\right]^2 \tag{49}$$

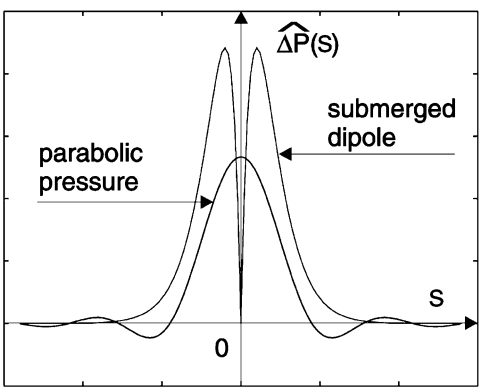

Fig. 7. Aspect of the $\hat{P}(s)$ for the submerged dipole and for the parabolic pressure distribution.

We can define a non-dimensional wave-resistance coefficient as $C_\omega = F_x/(\rho U^2 a)$ and

$$C_w = 16 P_M^2 \frac{[Ka \cos Ka - \sin Ka]^2}{(Ka)^3} \tag{50}$$

where $P_M = \overline{\Delta P}/(\rho g a)$. Defining the Froude number as $Fr = U\sqrt{ga}$, then $Ka = 1/Fr^2$. In Fig. 8 we show the plot of the analytical wave-resistance coefficient as a function of the Froude number, compared with a finite element computation detailed by Storti et al. (1998a,b).

5. The three dimensional case

The extension to the (symmetric) three dimensional case can be done by means of an additional Fourier transform in the transversal (beam) direction. The contribution to the wave-resistance of each mode can be computed with a contour integral similar to the one studied here, but with the simplification that for the non null transversal *m*-modes, the branch cuts on the imaginary axis do not cover the whole axis but, indeed, they extend for $|\mathrm{Im}(k)| > |M|$. This assertion can be shown as follows. The linearized governing system for $\phi(x, y, z)$ is now

$$\begin{cases} \phi_{,xx} + \phi_{,yy} + \phi_{,zz} = 0 & \text{in } z < 0; \\ \phi_{,z} + K^{-1}\phi_{,xx} = \psi, & \text{at } z = 0; \end{cases} \tag{51}$$

where $\psi(x,y,0) = U/(\rho g) P_{,x}$. We assume that ϕ, ψ are a linear combination of plane waves on x,y and for ϕ there is an exponential attenuation in z. Then, taking its Fourier transforms

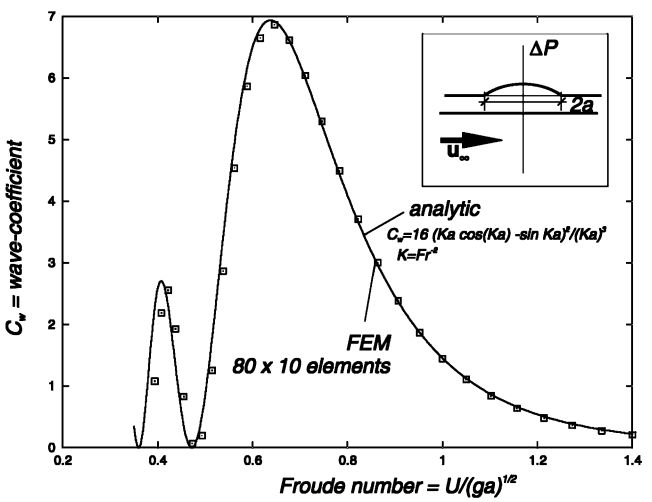

Fig. 8. Wave-resistance coefficient for a parabolic pressure distribution of compact support.

$$\phi = \int_{-\infty}^{\infty} dk \int_{-\infty}^{\infty} dm\, e^{ikx+imy+nz}\hat{\phi}; \tag{52}$$

$$\psi = \int_{-\infty}^{\infty} dk \int_{-\infty}^{\infty} dm\, e^{ikx+imy}\hat{\psi}; \tag{53}$$

where $n=n(k,m)$ is a dispersion relation that remains to be determined. Replacing Eqs. (52) and (53) in Eq. (51) we have

$$\begin{cases} (-k^2-m^2+n^2)\hat{\phi}=0 \ ; \\ (n-K^{-1}k^2)\hat{\phi}=\hat{\psi} \quad ; \end{cases} \tag{54}$$

eliminating n we find $\hat{\phi}=\hat{G}\hat{\psi}$, with the kernel

$$\hat{G}(k,m)=\frac{1}{\sqrt{k^2+m^2}-K^{-1}k^2}\ ; \tag{55}$$

this is singular at the points $k=\pm i|m|$ and $k=\pm K_m$ where

$$K_m=K\sqrt{1/2+1/2\sqrt{1+4m^2K^{-2}}}. \tag{56}$$

The singularities at $k=\pm i|m|$ can be linked by a branch-cut passing through infinite, so the integration path passes through a regular aperture on the imaginary axis, see Fig. 9, and in some way, the problem for $m\neq 0$ is more regular than the $m=0$ case. Lastly, the numerical solution of Eqs. (52) and (53), with kernel (55), can be computed with the discrete Fourier transform

$$\phi(I,J)=\sum_{k=1}^{N-1}\sum_{m=2}^{N-1}\frac{\hat{\psi}(k,m)W_N^{+kI}W_N^{+mJ}}{\sqrt{k^2+m^2}-K^{-1}k^2}\ ; \tag{57}$$

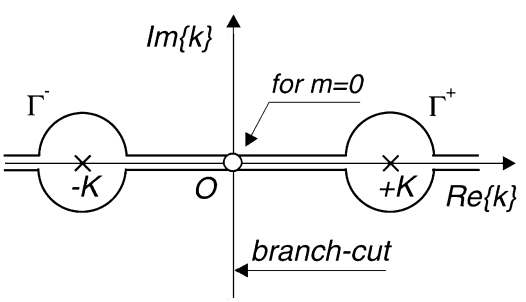

Fig. 9. The branch-cuts get farther away from the real axis as the beam Fourier m-modes increase.

for $I,J=0,1,\ldots,N-1$, where the contribution of the term $k=m=0$ is null, as mentioned in Section 2, N^2 is the total number of sample points and

$$\hat{\psi}(k,m)=\frac{1}{N^2}\sum_{I=0}^{N-1}\sum_{J=0}^{N-1}\psi(I,J)W_N^{-kT}W_N^{-mJ}; \tag{58}$$

for $k,m=1,2,\ldots,N-1$, where $W_N=\exp(2\pi i/N)$ is the weighting kernel. These computations can be efficiently implemented, for instance, through the Fast Fourier Transform. On the other hand, the dispersion relation given by Eq. (56) is a key term for an inexpensive computation of the wave pattern far downstream, like ten or 15 ship-lengths, and it is detailed in a previous work, see D'Elía et al., 2000a.

6. Conclusions

The overall approach is limited by the restrictions of the potential flow model, the use of a linearized free surface boundary condition and the replacement of the body by its equivalent pressure disturbance on the unperturbed free surface. In the wave-resistance formula arrived by the Fourier transform, only the symmetric part contributes to its value. The analytical approach allows to consider additional test cases, whenever the Fourier transform of the pressure distribution can be done in closed form, like the parabolic pressure distribution of compact support. The extension to the (symmetric) three dimensional case can be done by means of an additional Fourier transform in the transversal (beam) direction, where the transversal Fourier modes are more regular and in practical cases it can be performed numerically by the Fast Fourier Transform. In the extension to the three dimensional case, a dispersion relation was found as a key element for an inexpensive computation of the wave-pattern far downstream.

Acknowledgements

This work was supported through grants CONICET-PIP-198/98 (Germen-CFD), SECyT-FONCyT-PICT-51 (Germen) and CAI+D-UNL-94-004024. The work was partially performed with the Free Software Foundation/GNU-Project resources.

Appendix A. Contribution of the antisymmetric and symmetric parts of G to the wave resistance

In fact, from Eqs. (24), (27) and (29) we have that the wave resistance is the sum of its symmetric and anti-symmetric parts $F_x=F_s+F_a$, where

$$F_{s/a}=\frac{U}{g}\int\int P(x)G_{s/a}(x-x')P(x')\,dxdx'. \tag{59}$$

But, interchanging the integration variables x and x' in the skew-symmetric term F_a, we see that

$$F_a = -\frac{U}{g}\int\int P(x')G_a(x'-x)P(x)\,dx'dx; \tag{60}$$

but since $G_a(-\xi) = -G_a(\xi)$ we have

$$F_a = \frac{U}{g}\int\int P(x')G_a(x-x')P(x)\,dx'dx; \tag{61}$$

thus, $F_a = -F_a$, so the unique solution is $F_x = 0$ and only the symmetric part G_s is relevant for the wave-resistance computation and given by Eq. (30). On the other hand, the symmetric part G_s is obtained as

$$G_s(\xi) = \frac{1}{2}[G(\xi) + G(-\xi)]; \tag{62}$$

For $G(-\xi)$, with the variable change $u = -s$, we have that

$$\begin{cases} ds = -du & ; \\ F(s) = -F(u) & ; \\ \exp(-is\xi) = \exp(iku) & ; \\ \int_{P^-} \rightarrow \int_{P^+} & ; \end{cases} \tag{63}$$

and then

$$G(-\xi) = \frac{1}{2\pi}\int_{p+} du\, F(u)e^{iu\xi}\,; \tag{64}$$

replacing Eqs. (28) and (64) in Eq. (62) we arrive to the contour integral

$$G_s(\xi) = \frac{1}{4\pi}\int_{\Gamma} dsF(s)e^{is\xi}\,; \tag{65}$$

where Γ is now the net path composed of $\Gamma = \Gamma^+ + \Gamma^-$, and Γ^+ are small circles around each pole, see Fig. 5. Next, from the residue theorem

$$G_s(\xi) = \frac{i}{2}(F^+ + F^-); \tag{66}$$

where

$$F^{\pm} = \mathrm{Res}\{F(s)e^{is\xi}, \pm K\} \tag{67}$$

We know that $e^{is}\xi$ is analytic on $\pm K$ and we write

$$\mathrm{Res}\{F(s)e^{is\xi},\pm K\}=e^{iK\xi}\mathrm{Res}\ \{F(s),\pm\ K\}; \tag{68}$$

and since $F(s)$ has isolated poles on $\pm K$, the residue can be expressed as

$$\mathrm{Res}\{F,\pm K\}=\lim_{s\to\pm K}(s\mp K)F(s); \tag{69}$$

but with the variable change $u=-s$

$$\mathrm{Res}\{F,-K\}=\lim_{u\to-K}(K-u)F(-u); \tag{70}$$

and observing from Eq. (26) that F is skew-symmetric, we have

$$\mathrm{Res}\{F,-K\}=\lim_{u\to K}(u-K)F(u); \tag{71}$$

and then

$$\mathrm{Res}\{F,-K\}=\mathrm{Res}\{F,+K\}; \tag{72}$$

From Eqs. (66), (67) and (72) the symmetric part G_s is written as Eq. (31).

References

Bonet, R., Nigro, N., Storti, M., Idelsohn, S., 1998. A discrete non-local (DNL) out-going boundary condition for diffraction of surface waves. Commun. Numer. Methods Eng. 14, 849–861.

Chang, A.T., Chwang, A.T., 1997. Ship waves on a viscous fluid of finite depth. Phys. Fluids 9 (4), 940–944.

D'Elía, J., Storti, M., Idelsohn, S., 2000a. Smoothed surface gradients for panel methods. Adv. Eng. Software 31 (5), 327–334.

D'Elía, J., Storti, M., Idelsohn, S., 2000b. A closed form for low order panel methods. Adv. Eng. Software 31, 335–341.

D'Elía, J., Storti, M., Idelsolm, S., 2000c. Iterative solution of panel discretizations for potential flows the modal/multipolar preconditioning. Int. J. Num. Meth. Fluids 32, 1–27.

D'Elía, J., Storti, M., Idelsohn, S., 2000d. A panel-Fourier method for free-surface flows. ASME-J. Fluids Eng. 122, 309–317.

D'Elía, J., 1997. Numerical methods for the ship wave-resistance problem. Ph.D. Thesis, Universidad National de1 Litoral, Santa Fe, Argentina.

Doctors, L., Renilson, M., Parker, G., Hornsby, N., 1991. Waves and wave resistance of a high-speed river catamaran. In: FAST'SI, Trondheim., pp. 35–52.

Inui, T., 1962. Wave-making resistance of ships. Trans. Soc. Naval Archit. Mar. Eng. 70, 282–326.

Karp, S., Kotik, J., Lurye, J., 1960. On the problem of minimum wave resistance for struts and strut-like dipole distributions. In: Third Symposium on Naval Hydrodynamics, Scheveningen, pp. 56–110.

Lamb, H., 1945. Hydrodynamics, sixth ed. Dover Inc, New York.

Landweber, L., 1961. Motion of immersed and floating bodies. In: Streeter, V.L. (Ed.), Handbook of Fluid Dynamics. McGraw-Hill.

Larsson, L., Baba, E., 1996. Ship resistance and flow computations. In: Advances in Marine Hydrodynamics. Computational Mechanics Publications, Southampton, Boston.

Letcher, J.S., 1993. Properties of finite-difference operators for the steady-wave problem. J. Ship Res. 37 (1), 1–7.

Maruo, H., Bessho, M., 1963. Ships of minimum wave resistance. J. Zosen Kiokai 114, 9–23. Translated in Selected Papers 3, 1–8.

Miloh, T., 1991. Mathematical Approaches in Hydrodynamics. SIAM, Philadelphia.
Min, K.S., 1992. Design and construction of the long-range high speed foil-catamaran passenger ship. In: 19th Symposium on Naval Hydrodynamics, Seoul, Korea.
Mokry, M., 1990. Complex variable boundary element method for external potential flows. In: 28th Aerospace Sciences Meeting, Reno, Nevada.
Morino, L., 1985. Computational Methods in Potential Aerodynamics. Springer-Verlag.
Newman, J.N., 1976. Linearized wave resistance theory. In: Proceedings of International Seminar on Wave Resistance, Tokyo., pp. 31–43.
Noblesse, F., Gagan, G., 1976. Nonlinear ship-wave theories by continuous mapping. J. Fluid Mech. 75 (Part 2), 347–371.
Ogilvie, F., 1968. Wave resistance: the low speed limit. Rep. 002, Department of Naval Architecture and Marine Engineering, University of Michigan.
Ohkusu, M. (Ed.), 1996. Advances in Marine Hydrodynamics. Computational Mechanics Publications, Southampton, Boston.
Papanikolaou, A., Androulakakis, M., 1991. Hydrodynamic optimization of high-speed SWATH. In: FAST'91, Trondheim, pp. 507–522.
Raven, H.C., 1996. A solution method for the nonlinear ship wave resistance problem. Doctoral Thesis, Technical University Delft, Maritime Research Institute Netherlands (MARIN).
Stoker, J.J., 1957. Water Waves. Interscience Publishers, New York.
Storti, M., D'Elía, J., Idelsohn, S., 1995. CVBEM formulation for multiple profiles and cascades. Appl. Mech. Rev. 48 (11 (Part 2)), 203–210.
Storti, M., D'Elía, J., Idelsohn, S., 1998a. Algebraic discrete non-local (DNL) absorbing boundary condition for the ship wave resistance problem. J. Comp. Phys. 146, 570–602.
Storti, M., D'Elía, J., Idelsohn, S., 1998b. Computing ship wave resistance from wave amplitude with the DNL absorbing boundary condition. Commun. Numer. Methods Eng. 14, 997–1012.
Storti, M., D'Elía, J., Bonet Chaple, R., Nigro, N., Idelsohn, S., 2000. The DNL absorbing boundary condition. Applications to wave problems. Comp. Meth. Appl. Mech. Eng. 182, 483–498.
Suzuki, K., 1993. Fundamental study on optimum position of outriggers of trimaran from view point of wave making resistance. In: FAST'93, Yokohama, pp. 1219–1230.
Wehausen, J.V., Laitone, E.V., 1960. Surface waves. In: Handbuch der Physik, Vol. 9. Springer-Verlag, Berlin, pp. 446–778.
Wehausen, J.V., 1973. The wave resistance of ships. Adv. Appl. Mech. 13, 93–245.
Weinblum, G., 1930. Schiffe geringsten Widerstands. In: Proceedings of the 3rd International Congress of Applied Mechanics, Stockholm, pp. 449–458.
Wyatt, D.C., Chang, P.A., 1994. Development and assessment of a total resistance optimized bow for the AE36. Marine Technology 31, 149–160.